Solving stochastic inverse problems for cfd using data-consistent inversion and an adaptive stochastic collocation method

Hector Galante, Anca Belme, Jean-Camille Chassaing, Timothy Wildey

SOLVING STOCHASTIC INVERSE PROBLEMS FOR CFD USING DATA-CONSISTENT INVERSION AND AN ADAPTIVE STOCHASTIC COLLOCATION METHOD

H. Amino,[1] A-C. Belme,[2,*] J-C. Chassaing,[2] & T. Wildey[3]

[1]*Fluid Mechanics, Energy and Environment department (MFEE) , EDF R&D, Chatou, France*
[2]*Sorbonne University, CNRS, Institut Jean Le Rond d'Alembert, F-75005 Paris, France*
[3]*Computational Mathematics Department, Sandia National Laboratories, Albuquerque, USA*

*Address all correspondence to: A-C. Belme, Sorbonne University, CNRS, Institut Jean Le Rond d'Alembert, F-75005 Paris, France, E-mail: anca-claudia.belme@sorbonne-universite.fr

Original Manuscript Submitted: ; Final Draft Received: mm/dd/yyyy

The inverse problem we consider takes a given model and an observed (or target) output probability density function (pdf) on quantities of interest, and builds a new model input pdf which is consistent with both the model and the data in the sense that the push-forward of this pdf through the model matches the given observed pdf. However, model evaluations in CFD tend to require significant computational resources which makes solving stochastic inverse problems in CFD is very costly. To address this issue, we present a non-intrusive adaptive stochastic collocation method coupled with a data-consistent inference framework to efficiently solve stochastic inverse problems in computational fluid dynamics (CFD). This surrogate model is built using an adaptive stochastic collocation approach based on a stochastic error estimator and simplex elements in the parameters space. The efficiency of the proposed method is evaluated on analytical test cases and two CFD configurations. The metamodel inference results are shown to be as accurate as crude Monte Carlo inferences while performing 10^3 *less deterministic computations for smooth and discontinuous response surfaces. Moreover, the proposed method is shown to be able to reconstruct both an observed pdf on the data and key components of a data-generating distribution in the uncertain parameter space.*

KEY WORDS: *inverse problems, data-consistent, updated density, stochastic collocation, adaptive simplex, CFD, error estimation*

1. INTRODUCTION

The recent development of data-driven approaches has increased interest in developing robust and efficient algorithms to exploit data in engineering design and modelling in CFD. Often, one seeks to use data to improve models for a better understanding of the physical processes to enable more robust risk management. A common set of data d can be some function (usually experimental) of a system output also called *observed data*, or some desired (targeted) data, i.e., as is often used in optimization processes. A frequent question then arises: *what should be the model input that gives as output the targeted or observed data*. This is an inverse problem, and in an ideal environment, the solution to such problems would provide answers to unknown processes. However, solving such inverse problems using a high-fidelity CFD model is very expensive in computational time and storage. This cost is even more important if the CFD model is subject to uncertainties. Indeed, in practice, we are often interested in a model output, defined as a quantity of interest (QoI) whose value, while in presence of uncertainties, will no longer be a scalar but a functional depended on the uncertain parameters (i.e. a multi-dimensional functional). Besides the cost

2152–5080/17/$35.00

of high-fidelity CFD problems in presence of numerical uncertainties, the model must accurately describe highly nonlinear flow dynamics (like shock waves, turbulence, etc).

For forward problems, the Monte-Carlo (MC) method is the most common approach to quantify uncertainties. However, despite its robustness, ease of implementation and parallelization, MC methods quickly become infeasible for CFD applications due to their high computational cost. Other approaches rely on using the high-fidelity model to construct a surrogate, or metamodel, for the purposes of forward or inverse propagation of uncertainties. Examples include the generalized Polynomial Chaos (gPC) [1] methods which construct a parameterized polynomial approximation of the QoI response or the Stochastic Collocation (SC) methods which consist in constructing interpolation functions for given coefficients/samples [2,3]. All of these methods are highly efficient when the QoI $\boldsymbol{Q}(\boldsymbol{\lambda})$ response is sufficiently smooth. However, in the case where the stochastic response is of low regularity or even exhibit discontinuities, these global polynomial approximations are not amenable and may suffer from Gibbs oscillations. For instance, the propagation of changing operating conditions and variations in the geometry of compressible flows is well documented [4,5], but particularly challenging, e.g. [6]. This is because such systems are described by nonlinear conservation laws containing uncertain parameters and resulting in stochastic solutions with discontinuities in *both* physical and parametric dimensions. As each sample in the parameter space corresponds to a costly CFD simulation, it becomes mandatory to reduce as much as possible the number of needed samples in order to reach a prescribed QoI statistical accuracy. Therefore, *adaptive* solution techniques [7–13] represent alternative approaches that may guarantee and accelerate the convergence of the approximations, thanks to local relevant refinements of the response surface.

For inverse problems, Bayesian methods [14,15] are the most widely known approaches for inferring probabilistic descriptions of model parameters from data. These approaches rely on a fundamental theoretical result, known as Bayes' theorem, which provides a way to revise existing predictions given new or additional evidences.

The Bayesian approach is most commonly applied in scenarios where the model inputs are described as epistemic uncertainties with some prior probability distribution, and the goal is to determine the most likely model inputs that could have produced the observed data given a likelihood model. The choice of prior distribution reflects the prior knowledge or assumptions about the inputs being estimated and can have a significant impact on the inference results. A common approach for accelerating Bayesian inference in computationally intensive inverse problems relies on using forward surrogates models, constructed through repeated forward simulations (see for instance [6,16–18]). Moreover, in some pioneering works, such as those of [19] and [16], authors have pointed out that discontinuous solutions in the physical and stochastic spaces often lead to a propagation of error to the input parameter posterior distribution. This led to adaptive solutions for forward surrogate models coupled with the Bayesian approach, such as the use of iterative gPC in [6], locally adaptive multi-fidelity gPC approach in [20] or building an adaptive surrogate using goal-oriented a posteriori error estimate for quantities of interest in [21].

In this paper, we solve a different stochastic inverse problem where we seek an *aleatoric* characterization of the model inputs given an observed/target probability measure/density on quantities of interest. Such an aleatoric characterization is appropriate for problems where the variability in the observed data is due to intrinsic variability in the input parameters. In this scenario, the goal is to describe this variability on model inputs by seeking a probability measure/density on model inputs such that the corresponding push-forward measure/density matches the observed, or target, measure/density. Thus, we seek a pull-back probability measure. While pull-back measures are not necessarily unique, i.e., the inverse problem is not necessarily well-posed, the data-consistent approach introduced in [22,23] and applied to different studies [24–26] provide a robust and stable mechanism for constructing a pull-back measure by regularizing the problem in a manner similar to Bayesian inference.

The main objective in this paper is to combine the data-consistent inverse method of [22,23] with the metric-based stochastic adaptive collocation method introduced in [27] for surrogate computation. The stochastic adaptive approach of [27] consists in building adaptively a surrogate or metamodel by solving

a stochastic optimization problem in the uncertain parameters space. Indeed, we seek an optimal partitioning (or metric) of the parametric space (i.e. a "mesh") such that a prescribed stochastic error is minimized under the constraint of a computational cost (number of CFD computations one can afford). The surrogate/metamodel is then built on the probabilistic space using a stochastic collocation approach on these simplex elements. Among other adaptive approaches, this novel method has the advantage of being anisotropic, thus capable of accurately and automatically capturing discontinuities that may arise in the stochastic space. We study the performance of the combined methods applied to solving inverse stochastic propagation for CFD problems where the fluid flow is highly non-linear, compressible and in presence of discontinuities. Previous work combining surrogate, or approximate models, with data-consistent inversion, e.g., [25,28], require fairly strong assumptions about the convergence of the approximate map which may not hold for CFD applications where the true and surrogate maps may be discontinuous. Moreover, these previous works did not seek to incorporate adaptive surrogate/metamodels.

The remainder of this paper is organized as follows. We first define the stochastic inverse problem and provide the corresponding notation. Next, we introduce the data-consistent approach used to solve the stochastic inverse problem. In the fourth section, we briefly recall the adaptive simplex stochastic collocation (ASSC) approach proposed in [27]. The next section is dedicated to the verification of the proposed method on an academic problem with discontinuities. Finally, two CFD inverse problems featuring a NACA0012 airfoil and a scramjet geometry are solved using the proposed method. Some perspectives and conclusions are contained in the final section of this paper.

2. NOTATION AND INVERSE PROBLEM SETUP

In this section, we introduce our notation and summarize the mathematical framework of the stochastic inverse problem we seek to solve. Let $\Lambda \subset \mathbb{R}^n$ denote the space of model inputs, which we refer to as either the physical parameters or parameters of interest. Let $Q : \Lambda \to D \subset \mathbb{R}^m$ denote the quantity of interest (QoI) map from the physical parameters to the space of observable model output data denoted by $D \subset \mathbb{R}^m$. We assume in this work $(\Lambda, \mathcal{B}_\Lambda, \mu_\Lambda)$ and $(D, \mathcal{B}_D, \mu_D)$ are two measurable spaces on some Borel σ-algebras $\mathcal{B}_\Lambda$ restricted to Λ and respectively $\mathcal{B}_D$ on D. We assume that Q defines a measurable mapping between the two previously defined measure spaces i.e. Q is at least piecewise-smooth in D. Thus, for any event $A \in \mathcal{B}_D$, the measurability of Q implies that the contour σ-algebra is a sub-σ-algebra of $\mathcal{B}_\Lambda$, i.e.

$$Q^{-1}(A) = \{\boldsymbol{\lambda} \in \Lambda | \boldsymbol{Q}(\boldsymbol{\lambda}) \in A\} \in \mathcal{B}_\Lambda,$$

which implies

$$Q(Q^{-1}(A)) = A.$$

Next, assume we are given an observed (or target) probability measure $\mathbb{P}_D^{\text{obs}}$ on $(D, \mathcal{B}_D, \mu_D)$, that is absolutely continuous with respect to the measure μ_D and thus, thanks to the Radon Nykodim theorem, admits an observed probability density π_D^{obs}. This observed density may be approximated using physical data, given analytically as a target density, or constructed using a data-generating distribution on the model inputs which is propagated through the model to give π_D^{obs}. In this paper, we consider observed densities given analytically or constructed using the push-forward of a data-generating distribution on the input parameters. For the sake of simplicity, we do not consider errors in the observed density due to finite sampling or measurement error.

The implicit assumption here is that the variability in the observations is due to intrinsic variability of the model input parameters, i.e., we seek an aleatoric characterization of the model inputs.

The inverse problem seeks a probability measure denoted P_Λ on $(\Lambda, \mathcal{B}_\Lambda)$, absolutely continuous with respect to the measure μ_Λ such that the propagation of this measure/density through the model (i.e., the push-forward) matches the observed measure for all $A \in \mathcal{B}_D$. This push-forward measure/density is the solution to a forward uncertainty quantification problem that may be constructed or approximated before

any data is collected. If we let $\mathbb{P}_D^{Q(\mathbb{P}_\Lambda)}$ denote the push-forward (or predicted) probability measure of $\mathbb{P}_\Lambda$ through $\boldsymbol{Q}(\boldsymbol{\lambda})$, then we have

$$\mathbb{P}_D^{Q(\mathbb{P}_\lambda)}(A) = \mathbb{P}_\Lambda(Q^{-1}(A)),\ \forall A \in \mathcal{B}_D.$$

Then, we can formalize the definition of the inverse problem solved in this paper as follows: given an observed probability measure, $\mathbb{P}_D^{\text{obs}}$, we seek a $\mathbb{P}_\Lambda$ such that:

$$\mathbb{P}_D^{Q(\mathbb{P}_\lambda)}(A) = \mathbb{P}_\Lambda(Q^{-1}(A)) = \mathbb{P}_D^{obs}(A),\ \forall A \in \mathcal{B}_D. \tag{1}$$

We refer to any $\mathbb{P}_\Lambda$ that satisfies (1) as a *data-consistent* solution to the inverse problem. Of course, there are typically infinitely* many probability measures that satisfy (1). In the next section, we describe a procedure that uses prior information to regularize the inverse problem such that an unique, stable and computable solution to the inverse problem may be obtained.

3. A SOLUTION TO THE STOCHASTIC INVERSE PROBLEM

Let $\mathbb{P}_\Lambda^{\text{init}}$ on $(\Lambda, \mathcal{B}_\Lambda, \mu_\Lambda)$ be an initial probability measure on model inputs that is absolutely continuous with respect to μ_Λ and with a probability density function $\pi_\Lambda^{\text{init}}$. This initial measure/density is linked to the existing knowledge that we have regarding the aleatoric uncertainty in the parameters of interest. For the ease of notation, we use $\mathbb{P}_D^{Q(\text{init})}$ and $\pi_D^{Q(\text{init})}$ to denote the push-forward measure and respectively density of the initial measure through the model, i.e., these denote the *initial prediction*. The goal is to update this initial measure to give a solution to the stochastic inverse problem.

However, in order to obtain a data-consistent solution to this problem, we must ensure that $\pi_D^{Q(init)}$ exists with respect to μ_D and that the inverse problem is solvable. Following [22], the former can be assured if the volume measure, μ_D, is chosen properly. For the latter, we need to make the following assumption:

Assumption 1 (predictability) : There exists a constant C > 0 such that $\pi_D^{obs}(q) \leq C\pi_D^{Q(init)}$ for almost every $q \in D$.

Assumption 1 implies that the observed measure is absolutely continuous with respect to the predicted measure in D. This assumption can be interpreted as ensuring that the push-forward of the initial probability measure through the model can predict all the observed data. If this is not the case, then there is no way to update the initial to obtain a solution to the inverse problem.

In [22] it is shown that a unique and stable solution can be obtained using the disintegration theorem [29]. For the sake of completeness, we restate this theorem here:

Disintegration Theorem : Assume $Q : \Lambda \to D$, $\mathcal{B}_\Lambda$ measurable, P_Λ is a probability measure on $(\Lambda, \mathcal{B}_\Lambda)$ and P_D is the push-forward measure of P_Λ on $(D, \mathcal{B}_D)$. There exists a probability measure P_D -almost everywhere uniquely defined by a family of conditional probability measures $\{P_q\}_{q\in D}$, on $(\Lambda, \mathcal{B}_\Lambda)$ such that for any $A \in \mathcal{B}_\Lambda$,

$$P_q(A) = P_q(A \cap Q^{-1}(q)).$$

Therefore, P_Λ can be written as an integral

$$P_\Lambda(A) = \int_D P_q(A) dP_D(q) = \int_D \left(\int_{A\cap Q^{-1}(q)} dP_q(\lambda) \right) dP_D(q),\ \forall A \in \mathcal{B}_\Lambda. \tag{2}$$

The Disintegration theorem plays a critical role in constructing solutions to this class of inverse problem as it decomposes the input parameter space into directions informed by the map/data and directions defined by generalized contours of the map over which $Q(\boldsymbol{\lambda})$ is constant. Any pullback probability measure (solution to the inverse problem) is required to be the inverse image of the observed measure in the

*Unless the QoI map is bijective, in which case, the solution is unique.

informed directions, while the conditional probability measure within the contour event, $A \cap Q^{-1}(q)$, can be any valid probability measure. As shown in [22], this theorem can be used to show that the updated probability measure $\mathbb{P}_\Lambda^{\text{up}}$ on $(\Lambda, \mathcal{B}_\Lambda)$ defined by

$$\mathbb{P}_\Lambda^{\text{up}}(A) = \int_D \left(\int_{A \cap Q^{-1}} \pi_\Lambda^{\text{init}}(\boldsymbol{\lambda}) \frac{\pi_D^{obs}(Q(\boldsymbol{\lambda}))}{\pi_D^{Q(\text{init})}(Q(\boldsymbol{\lambda}))} d\mu_{\Lambda,q}(\boldsymbol{\lambda}) \right) d\mu_D(q), \forall A \in \mathcal{B}_\Lambda, \tag{3}$$

solves the stochastic inverse problem. As discussed in [22], the iterated integral form of the updated measure, given in (3), is not required to approximate or generate samples from the updated density. Rather, the updated density is calculated from the initial probability density using:

$$\pi_\Lambda^{\text{up}}(\boldsymbol{\lambda}) = \pi_\Lambda^{\text{init}}(\boldsymbol{\lambda}) \frac{\pi_D^{obs}(Q(\boldsymbol{\lambda}))}{\pi_D^{Q(\text{init})}(Q(\boldsymbol{\lambda}))}. \tag{4}$$

This expression makes it clear why the solution to the stochastic inverse problem is called an *updated* measure/density, since the ratio of the observed and predicted densities is used to update (reweight) the initial probability density.

We conclude this section with a brief discussion of the similarities and differences between the probability density given in (4) and the classical Bayes formula. In a Bayesian formulation, the posterior probability density is defined as the prior probability density times the ratio of the likelihood and the evidence (integral of the likelihood with respect to the prior). Thus, both formulations are similar in the sense that they updated prior/initial characterizations using ratios of quantities dependent on the map and the observed data. However, prior and posterior probability densities represent epistemic characterizations of the relative probability that a given parameter may have produced the observed data. In the inverse problem discussed in this paper, the initial and updated densities represent aleatoric characterizations of the model inputs that are consistent with a given observed probability measure. In general, the two formulations give different solutions, and the choice of which to use depends on the inverse problem one wishes to solve.

3.1 Computational considerations

In this section, we provide the main steps in numerically estimating and generating samples from the updated probability density. First, we assume we have the ability to generate samples from $\pi_\Lambda^{\text{init}}$. A forward uncertainty propagation is performed by generating samples from $\pi_\Lambda^{\text{init}}$, evaluating the model (or metamodel/surrogate), and the push-forward density $\pi_D^{Q(\text{init})}$ can be estimated using a straightforward technique, such as Kernel Density Estimation (KDE). In Section 5, several methods for accelerating this forward propagation are investigated and performances compared. To generate samples from the updated density, a simple rejection sampling algorithm is applied using the samples generated from the initial. This computation is thus performed without the need of any additional deterministic calculations, which is extremely useful for computationally expensive CFD simulations.

For generalization and validation purposes we have investigated two different mechanisms for generating an observed/target density π_D^{obs}: (a) we define directly π_D^{obs} using classical analytical distributions (Gaussian, etc..), (b) we use the model, or metamodel, to build π_D^{obs} starting from a user-defined data-generating input density π_Λ^{obs} on the input parameters. Note that π_D^{obs} could also be provided or approximated using experimental data. However, the generation and incorporation of measurement data is beyond the scope of this work. The pre-processing steps of the data-generating method are illustrated in Algorithm 1 below. As we shall see in Sections 5 and 6, using a data-generating distribution allows us to make useful observations about the expectations that one should have when solving this class of inverse problems. In particular, it should only be possible to recover the data-generating distribution in a

lower-dimensional manifold induced by the map and the data. More precisely, in the under-determined case (more input parameters than observations) the updated density defines a unique solution on a lower dimensional manifold, but this solution can be combined with any conditional probability density defined within the generalized contours and still solve the stochastic inverse problem (see [22,30] for details). This is not necessarily a drawback of the proposed approach, rather, it is a feature of pull-back measures for under-determined maps.

Algorithm 1: *Synthetic computation of π_D^{obs} using a data-generating distribution.*

Generate N_0 samples from π_Λ^{obs} using a sampling method ;

Evaluate the QoI map $Q(\boldsymbol{\lambda})$ through a model or metamodel;

Compute π_D^{obs} using the Kernel Density Estimator ;

4. ADAPTIVE SIMPLEX STOCHASTIC COLLOCATION METHOD (ASSC)

This section aims to summarize the surrogate method (metamodel) used to accelerate the construction of the push-forward density of the quantity of interest, i.e. $\pi_D^{Q(\text{init})}$. As previously stated, we are interested in solving stochastic inverse CFD problems where discontinuities from the physical space might also propagate to the uncertain parameters space, meaning that the quantity of interest might have high and abrupt variations in the stochastic space. Moreover, we are also sensitive to the potentially high computational cost of each realization in the stochastic space. Using metamodels, which consists in building a response surface of the quantity of interest on the parameters of interest space from a limited number of realizations (i.e. CFD problems solves), is the solution we have considered in this paper.
Several methods have been proposed in the literature to deal with discontinuous response surfaces, such as: multi-wavelets basis projection on block partitions in [12], multi-element gPC in [31], iterative gPC in [6], ENO-type stencils and stochastic simplex collocation method in [32], minimal Multi-Element stochastic collocation in [11]. All of these approaches share the need for a discontinuity or solution regularity detector often considered using the local variance of the solution or a polynomial annihilation edge detection such as proposed in [13] and inspired by discontinuous physical solutions problems. Moreover, these approaches lack information regarding the anisotropic behavior of the discontinuity. We have chosen here to build the metamodel using the adaptive simplex stochastic collocation (ASSC) approach of [27,33] which uses the continuous framework of Riemannian metrics to construct anisotropic partition of the parameters domain. The main idea is to estimate the stochastic error on the quantity of interest measuring the difference between the true value and the value estimated from the metamodel utilizing an interpolation error estimate on the parameter space and use this error measure to refine the uncertain parameter space. This method is inspired from what is done for deterministic quantities of interest, where the computational (physical) mesh is adapted to improve the prediction of these quantities (see for example [34–36]). However, several differences appear when dealing with adaptivity in the stochastic/parametric space: (a) each "mesh" node is a costly CFD computation and (b) we need to account for the initial probability density. As it will be demonstrated later in the results section, using this method leads to anisotropic, accurate and less costly results compared to other classical metamodels or sampling methods for problems with sharp gradients or discontinuities.

The stochastic adaptive problem is formulated as an optimization problem in the parametric space. We formulate and solve this optimization problem using mathematical framework of the continuous Riemannian metric (RM) space [37,38]. The motivation for using this framework is twofold: using a continuous formulation such as the RM space allows us to have the proper mathematical framework for solving this

optimization problem and the solution to this problem provides anisotropic information which are very useful when dealing with discontinuities that do not necessarily run along the principal directions. More precisely, we use the RM space as a continuous model for the partition of the parametric space into simplex elements. From this continuous representation, a unit "mesh" is computed, for which the lengths of the element edges are (approximately) unity in the RM space. Upon transformation to a Euclidean space, i.e. our uncertain parameters space Λ, an anisotropic partition of Λ is obtained. Further details regarding the continuous framework of Riemannian metric space can be found in [37,38].

After construction of this partition of the parametric space, the stochastic response is approximated thanks to a tessellation of linear simplex elements, well adapted for discontinuous responses [39,40]. In this respect, it resembles the simplex stochastic collocation (SSC) method, which uses a similar discretization. In contrast, the method proposed in this work makes use of a stochastic error estimate committed in approximating the quantity of interest on this tessellation, or stochastic "mesh". Next, we describe the stochastic error estimate and the optimization problem, where we seek an optimal Riemannian metric in the parametric space. For a more detailed description of this problem, we refer to [27].

4.1 Stochastic error estimate and optimization problem

As previously mentioned, and in order to have an accurate solution to the inverse problem, we need also a good approximation of the push-forward of the initial density $\pi_D^{Q(\text{init})}$. The estimation of this density depends on how accurate we can predict the quantity of interest on the stochastic space. Using a continuous approximation, i.e. a metamodel, of the QoI on the stochastic space is an efficient solution to predict statistical information and new values of the QoI. However, we can only use a limited number of CFD computations, thus each sample needs to be chosen such that the prediction of the QoI is as accurate as possible. In this paper, we use a stochastic error estimation based on interpolation errors in the stochastic space. Let

$$\boldsymbol{Q}(\boldsymbol{\lambda}) = q\big(\boldsymbol{\lambda}, w(\boldsymbol{\lambda}, \mathbf{x})\big),$$

denote the quantity of interest which depends on the uncertain parameters $\boldsymbol{\lambda}$ and on the model solution $w(\boldsymbol{\lambda}, \mathbf{x})$ (for example the Navier-Stokes model solution) through an observation operator q. For the purpose of this paper, we neglect the deterministic discretization error for each realization of the QoI, meaning that in practice we evaluate an approximation of w which is assumed to be sufficiently accurate. We refer to [27] for a detailed description of the coupled deterministic-stochastic error control where mesh adaptivity has been used to minimize deterministic discretization errors. Suppose a discretization or partition $\mathcal{H}_h$ of the parametric space Λ into simplex elements using a finite number of samples $\boldsymbol{\lambda}_{(i)}$, $\forall i = 1, ..., ns$. A surrogate (or meta-) model is built from the computations on these samples. Then, let

$$\boldsymbol{Q}_h(\boldsymbol{\lambda}_{(i)}) = q_h\big(\boldsymbol{\lambda}_{(i)}, w(\boldsymbol{\lambda}_{(i)}, \mathbf{x})\big), \tag{5}$$

be the approximate stochastic response or approximate quantity of interest. We aim to provide an estimate of the following stochastic approximation error

$$\delta\boldsymbol{Q} \equiv \mathbf{Q} - \mathbf{Q}_h \tag{6}$$

For the type of applications we consider, it is nowadays common knowledge that the dependence of the QoI on the random variables (or parameters) is anisotropic, as we often encounter singularities and sharp response gradients. To this purpose, we follow and adapt the deterministic formulation in [41], in order to express the stochastic error using the L^p-norm of the interpolation error

$$\|q(\lambda_i, w) - \Theta_h q(\lambda_i, w)\|_{L^p(\Lambda)} \tag{7}$$

where Θ_h is the (linear) interpolation operator in the parameters space. For the purpose of this paper, we will focus on the L^1-norm of the interpolation error in the stochastic space Λ with associated measure μ_Λ.

This is a purely practical choice, well adapted for approximation of potentially discontinuous solutions, but there is no restriction in using a different p-norm. We highlight here that since the true interpolation error is not known, an *interpolation error model* is used to approximate the linear interpolation error as it will be explained in the next section.
For deterministic problems, this kind of approach named "feature" or "sensor"-based mesh adaptation has been proposed to capture all the scales/singularities of the model response and has been successfully applied to improve CFD models predictions [41,42]. Several differences appear naturally when employing this approach in the stochastic context. First, the *sensor* here is our quantity of interest $\mathbf{Q}$. Second, the L^1-norm of the interpolation error of $\mathbf{Q}$ on the parameter space, now equipped with a probability measure μ_Λ, introduces the input density $\pi_\Lambda^{\text{init}}$ in the formulation. Furthermore, $\delta\mathbf{Q}$ being a random quantity, we focus on minimizing the average error $\bar{\eta}$ where

$$\bar{\eta} = \mathbb{E}\left[\delta\mathbf{Q}\right] \leq \int_\Lambda |q(\boldsymbol{\lambda}_i, w) - \Theta_h q(\boldsymbol{\lambda}_i, w)| \pi_\Lambda^{\text{init}}(\boldsymbol{\lambda}) \mathrm{d}\mu_{\boldsymbol{\lambda}}. \tag{8}$$

We highlight here that the probability density function acts as a weighting of the interpolation error. The error estimate (8) will be used as refinement indicator to drive adaptivity over Λ. More precisely, our stochastic error control problem will be formulated as an *optimization problem*, which solution is an optimal discretization of the parameters space, minimizing the stochastic error (8) under the constraint of a given number of samples. A continuous formulation of this discrete optimization problem is proposed where a continuous error model for the interpolation error in the stochastic space is built using linear interpolation model in a Riemannian metric space. This error model and optimal solution will be expressed in terms of Hessians of Q in the parameters space as explained hereafter.

4.1.1 Stochastic Adaptive optimization problem

An efficient approach to generate anisotropic meshes in the physical deterministic space has been introduced in [37,38]. In order to build such meshes, one must be able to prescribe at each point of the computational domain privileged sizes and orientations for the elements. The use of Riemannian metric spaces is an elegant and efficient way to achieve this goal. The main idea of metric-based mesh adaptation, initially introduced in [43], is to generate a *unit mesh* in a prescribed Riemannian metric space. Consequently, the generated mesh will be uniform and isotropic in the Riemannian metric space while it will be anisotropic and adapted in the usual, Euclidean space. This approach will be used to generate anisotropic "meshes" in the uncertain parameters space.

The Riemannian metric spaces can be seen as continuous models representing meshes. Working in this framework allowed us to dispose of all the mathematical tools to define and solve the stochastic optimization problem defined in this section. Moreover, as shown in [37] there is a duality between the continuous framework of Riemannian metric spaces and the discrete space of our stochastic problem resolution. For all $\mathbf{x} \in \Omega \subset \mathrm{R}^n$, a Riemannian metric $\mathcal{M}(\mathbf{x})$ is a symmetric matrix having $(\xi_i(\mathbf{x}))_{i=1,\dots,n}$ as eigenvalues along the principal directions $(\mathbf{v}_i(\mathbf{x}))_{i=1,\dots,n}$. Sizes along these directions are denoted $(h_i(\mathbf{x}))_{i=1,\dots,n} = (\xi_i^{-\frac{1}{2}}(\mathbf{x}))_{i=1,\dots,n}$.
In the duality between the discrete and continuous space it is shown that discrete interpolation errors such as formulation (8) are well represented by the *continuous interpolation error* related to $\mathcal{M}$, which is expressed locally in terms of the Hessians as follows:

$$(q - \pi_{\mathcal{M}} q)(\mathbf{x}) \quad = \quad \frac{1}{10} \text{trace}(\mathcal{M}^{-\frac{1}{2}}(\mathbf{x}) \, |H_q(\mathbf{x})| \, \mathcal{M}^{-\frac{1}{2}}(\mathbf{x})) \tag{9}$$

where we denoted $q - \pi_{\mathcal{M}} q$ the continuous dual of the discrete interpolation error in (8) and $H_q(\mathbf{x})$ the Hessian matrix of $q(\mathbf{x})$.

Using this continuous framework of Riemannian metric space and the associated continuous error model (9), the stochastic error estimate (8) has the following representation in the Riemannian metric space

$$\mathbf{E}_{\boldsymbol{\lambda}}(\mathcal{M}) \;=\; \int_{\Lambda} \text{trace}\left(\mathcal{M}^{-\frac{1}{2}}(\boldsymbol{\lambda})\,\pi_{\Lambda}^{\text{init}}(\boldsymbol{\lambda})\cdot H(\mathbf{Q}(\boldsymbol{\lambda}))\,\mathcal{M}^{-\frac{1}{2}}(\boldsymbol{\lambda})\right)\,\mathrm{d}\mu_{\boldsymbol{\lambda}}, \tag{10}$$

with $H(\mathbf{Q}(\boldsymbol{\lambda}))$ the Hessian matrix of $\mathbf{Q}(\boldsymbol{\lambda})$.
The *stochastic optimization problem* is then formulated as follows:

$$\text{Find } \mathcal{M}_{\boldsymbol{\lambda}}^{opt} = \underset{\mathcal{M}_{\lambda}}{\text{argmin}}\ \mathbf{E}_{\boldsymbol{\lambda}}(\mathcal{M}), \quad \text{subject to} \quad \mathcal{C}(\mathbf{M}) = \mathcal{C}_{\boldsymbol{\lambda}}, \tag{11}$$

where $\mathcal{C}_{\boldsymbol{\lambda}}$ denotes a specified complexity in the parameters space, which is equivalent to the targeted number of samples (or CFD solver runs). This means that a targeted computational effort constraint is imposed. The notation $\mathcal{M}_{\boldsymbol{\lambda}}^{opt}$ holds for the optimal metric that minimizes the expectation of the continuous interpolation error in the parameter space. We will use this metric to build a simplex tessellation of the parameter space, which is, roughly the "mesh"† associated with Λ. The optimal stochastic metric, solution to the $n-$dimensional optimization problem (11) is

$$\mathcal{M}_{\boldsymbol{\lambda}}^{opt} = \mathcal{C}_{\boldsymbol{\lambda}}^{\frac{2}{n}} \left(\int_{\Lambda} \det(\pi_{\Lambda}^{\text{init}}(\boldsymbol{\lambda})|H(\mathbf{Q}(\boldsymbol{\lambda}))|)^{\frac{1}{2+n}} d\mu_{\boldsymbol{\lambda}}\right)^{-\frac{2}{n}} \det(\pi_{\Lambda}^{\text{init}}(\boldsymbol{\lambda})|H(\mathbf{Q}(\boldsymbol{\lambda}))|)^{-\frac{1}{2+n}} |\pi_{\Lambda}^{\text{init}}(\boldsymbol{\lambda}) H(\mathbf{Q}(\boldsymbol{\lambda}))| \tag{12}$$

and the error estimate on this optimal metric is given by

$$\mathbf{E}_{\boldsymbol{\lambda}}^{opt}(\mathcal{M}_{\boldsymbol{\lambda}}^{opt}) = n\mathcal{C}_{\boldsymbol{\lambda}}^{-\frac{2}{n}} \left(\int_{\Lambda} \det(\pi_{\Lambda}^{\text{init}}(\boldsymbol{\lambda})|H(\mathbf{Q}(\boldsymbol{\lambda}))|)^{\frac{1}{2+n}} \mathrm{d}\mu_{\boldsymbol{\lambda}}\right)^{\frac{2+n}{n}}. \tag{13}$$

The proofs for formulations (12) and (13) are included in [33].

4.1.2 Stochastic adaptive strategy

We emphasize here that we rely on non-intrusive methods for the approximation of the stochastic problem, meaning that the deterministic solver counterpart (e.g. the CFD code) is seen as a black box. Many different choices of non-intrusive stochastic surrogate models are available prior to the sampling adaptation. However, for our type of applications, it is necessary to rely on methods that are *robust*, i.e. relatively insensitive to the response surface smoothness, *flexible* and *efficient*, i.e. with an easy handling of local parametric sampling avoiding tensor-based refinements. The Simplex-Stochastic Collocation (SSC) method is a good candidate that meets these requirements by discretizing the domain into simplices, and naturally enforces local extrema conservation to suppress non-physical oscillations. A simple piecewise-linear approximation is chosen over higher degree polynomial approximation in accordance with the error estimate chosen to drive the "mesh" adaptation in the parameter space. Indeed, the error estimate is based on the interpolation error committed when linearly interpolating a quadratic function.

The adaptive response surface in the parameter space is generated using similar numerical tools to the deterministic case. Barring a few differences, a fixed-point algorithm is also used here. In the stochastic case, since each mesh vertex (sample) truly represents a (potentially) costly CFD simulation, samples acquired along the adaptation steps are always kept in the final discretization and we allow only the addition of new samples or connections swap between samples. In this case, the cumulative sum of mesh vertices from the initial design up to the final mesh is relevant to the numerical cost of the approximation method. The adaptive metamodel construction and the estimation of $\pi_D^{Q(\text{init})}$ are summarized in Algorithm 2.

†Here the "mesh" nomenclature is used as a generic term for sampling and related discretization of the parametric space.

Algorithm 2: Adaptive metamodel construction and $\pi_D^{Q(\text{init})}$ computation

- Given a set of $N_{\boldsymbol{\lambda},0}$ initial samples $\{\boldsymbol{\lambda}_i\}_0$ form the initial mesh $\mathcal{H}_{\boldsymbol{\lambda},0}$ using a Delaunay triangulation ;
- Evaluate the model to compute $\boldsymbol{Q}(\{\lambda_i\}_0)$;

For $l = 1$ **to** n_{adap} ;

► Compute optimal metric $\mathcal{M}_{\boldsymbol{\lambda}_i,l}^{opt}$ and the stochastic error, solutions of the stochastic optimization problem (11) with given complexity value $\mathcal{C}_{\boldsymbol{\lambda}}$ based on the QoI evaluation on the (vertices of the) previous mesh $\mathcal{H}_{\boldsymbol{\lambda},l-1}$;

► Use anisotropic information provided by the metric to generate new mesh $\mathcal{H}_{\boldsymbol{\lambda},l}$ containing $N_{\boldsymbol{\lambda},l} = N_{\boldsymbol{\lambda},l-1} + N_{\boldsymbol{\lambda},l}^{new}$ samples;

► Use model to compute the QoI at the $N_{\boldsymbol{\lambda},l}^{new}$ new samples and update the metamodel $\boldsymbol{Q}(\{\boldsymbol{\lambda}\}_l)$ using linear interpolation (stochastic collocation approach);

► If needed, compute the statistical moments of the metamodel;

EndFor ;

- Generate a large number of samples from $\pi_\Lambda^{\text{init}}$ and evaluate metamodel at each sample;
- Use a standard technique such as a kernel density method to estimate $\pi_D^{Q(\text{init})}$;

As outlined in Algorithm 2, we start out by (randomly) sampling Λ using $\pi_\Lambda^{\text{init}}$ and constructing an initial mesh as a Delaunay triangulation with samples λ_i. The model is evaluated for each of these samples and QoI information is extracted. We then solve iteratively (as a fixed-point iteration) the stochastic optimization problem (11) which has the optimal metric (12) as solution. We have used our in-house solver `METRIX` [44] for the optimal metric computation. `METRIX` uses the QoI information provided by the model (CFD solver) at each mesh point as well as the mesh file to first compute the Hessian matrix $H(\boldsymbol{Q}(\boldsymbol{\lambda}))$ using derivative recovery methods such as L^2-projection or Green formula, then the optimal metric $\mathcal{M}_{\lambda_i,l}^{opt}$ for each λ_i is assembled. We recall the optimal metric is the solution of a N-constrained optimization problem, where N is the maximum number of model evaluations we can afford. Therefore, at each iteration in the fixed point loop, the position of the new samples generated and the connection of these samples with the previous triangulation is decided by the optimal metric such as the stochastic error is minimized. The model is evaluated on those samples to extract QoI information and the new stochastic mesh is generated using a deterministic anisotropic mesh generator tool `FEFLO` (see for example [45]). We highlight here that the optimal metric takes into account additional information, i.e. $\pi_\Lambda^{\text{init}}$. At the end of the fixed point loop, when $l = n_{adap}$ we have obtained our metamodel with a computational cost controlled by the constraint.

The push-forward density $\pi_D^{Q(\text{init})}$ is then computed using a kernel density estimator (KDE) combined with a sampling method such as Monte-Carlo (MC) or Latin Hypercube Sampling (LHS). Although other methods can be used to compute this density, we have chosen to use a KDE for the sake of simplicity and reproducibility. We are now able to compute the updated probability density π_Λ^{up} for any $\boldsymbol{\lambda} \in \Lambda$ using relation (4) where $\pi_D^{Q(\text{init})}$ has been computed using Algorithm 2. However, it is common practice when solving stochastic inverse problems to simply generate samples from π_Λ^{up} using a basic rejection sampling algorithm on the samples generated from $\pi_\Lambda^{\text{init}}$. For details on this rejection sampling strategy, see [22].

5. VERIFICATION

The new strategy of solving stochastic inverse CFD problems using data-consistent inversion and the adaptive simplex collocation method is tested in this section. We focus on the verification of the proposed method on an analytical problem previously studied in [22] who presents a discontinuous QoI response surface.

The influence of the metamodel choice is also investigated in this section.

The test function is a $n-$dimensional piece-wise continuous function which is setup to be our QoI. A discontinuous representation of $\boldsymbol{Q}(\boldsymbol{\lambda})$ on parameters space Λ is considered here and illustrated for 2-dimensional case in Figure 1 (left image). This problem is meant to illustrate some of the issues we might encounter when dealing with compressible CFD problems, where discontinuities can arise in the QoI response.

We define

$$\boldsymbol{Q}(\boldsymbol{\lambda}) = \begin{cases} Q_1(\boldsymbol{\lambda}) - 2 \text{ if } \ 3\lambda_1 + 2\lambda_2 \geq 0 \text{ and } \ -\lambda_1 + 0.3\lambda_2 < 0 \\ 2Q_2(\boldsymbol{\lambda}) \quad \text{if } \ 3\lambda_1 + 2\lambda_2 \geq 0 \text{ and } \ -\lambda_1 + 0.3\lambda_2 \geq 0 \\ 2Q_1(\boldsymbol{\lambda}) + 4 \text{ if } \ (\lambda_1+1)^2 + (\lambda_2+1)^2 < 0.95^2 \text{ and } n = 2 \\ Q_1(\boldsymbol{\lambda}) \qquad\qquad\qquad\qquad \text{otherwise,} \end{cases}$$

with

$$Q_1(\boldsymbol{\lambda}) = exp(-\sum_{i=1}^{n} \lambda_i^2) - \lambda_1^3 - \lambda_2^3; \ Q_2(\boldsymbol{\lambda}) = 1 + Q_1(\boldsymbol{\lambda}) + \frac{1}{4n}\sum_{i=1}^{n} \lambda_i^2,$$

with uncertain parameters $\boldsymbol{\lambda} = [\lambda_1, \lambda_2, ..., \lambda_n]$, $n \in N$. For visualization purposes, we focus on $n = 2$ and $\boldsymbol{\lambda} \in \Lambda = [-1, 1]^2$. The observed probability density is built from an initial normal distribution $\pi_\Lambda^{\text{obs}}(\boldsymbol{\lambda}) = \mathcal{N}([0.2, 0.7], [0.03^2, 0.005^2])$ with mean and variance values 0.2 and 0.3 for λ_1 and respectively 0.7 and 0.005 for λ_2 such that it is defined on the threshold between two piecewise continuous surfaces as shown on Figure 1 (a) and respectively Figure 1 (b), where the samples from π_Λ^{obs} are drawn. The resulting observed QoI density is illustrated in Figure 1 (c). We investigate the solution to the stochastic inverse problems using two different metamodels: a generalized polynomial chaos approach (gPC) with 5th order polynomial approximation and our ASSC method.

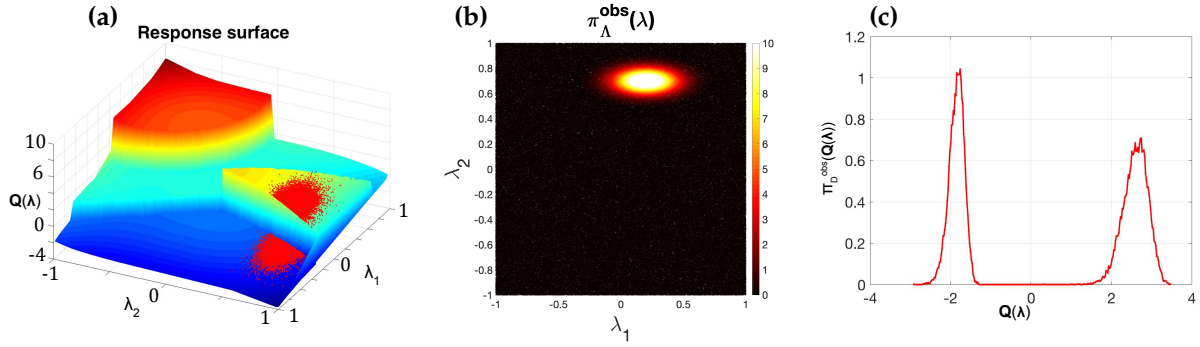

FIG. 1: *Verification. Reference densities in Λ and D stochastic spaces. (a) QoI response surface and samples generated from the initial support distribution π_Λ^{obs}, (b) initial support distribution π_Λ^{obs} used to built the observed data density. (c) The observed (targeted) density π_D^{obs}.*

We consider initially the two uncertain parameters to be uniformly distributed (i.e. $\pi_\Lambda^{\text{init}}$ follows a uniform distribution law on Λ). The resulting metamodels obtained using 5th order gPC and our ASSC adaptive approach are illustrated in Figure 2. We remark the global polynomial approximation is unable to accurately capture the discontinuities in the QoI definition, which is essentially expected, while the metamodel obtained using the ASSC with the same number of deterministic samples is capable to accurately

and automatically capture these discontinuities. A number of 10^5 post-processing LHS samples are used over the metamodels to infer the observed data.

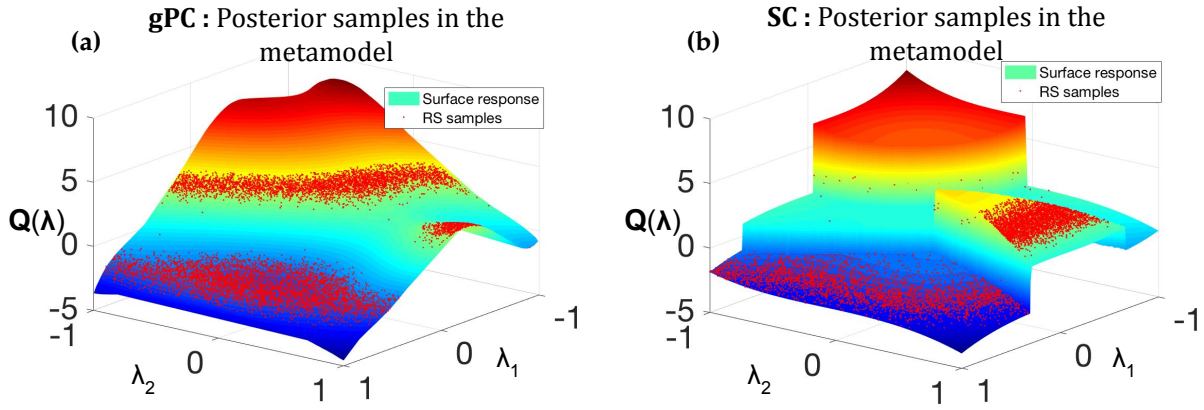

FIG. 2: *Verification. Response surface of the QoI for each metamodel with the updated density samples (a) gPC (b) ASSC.*

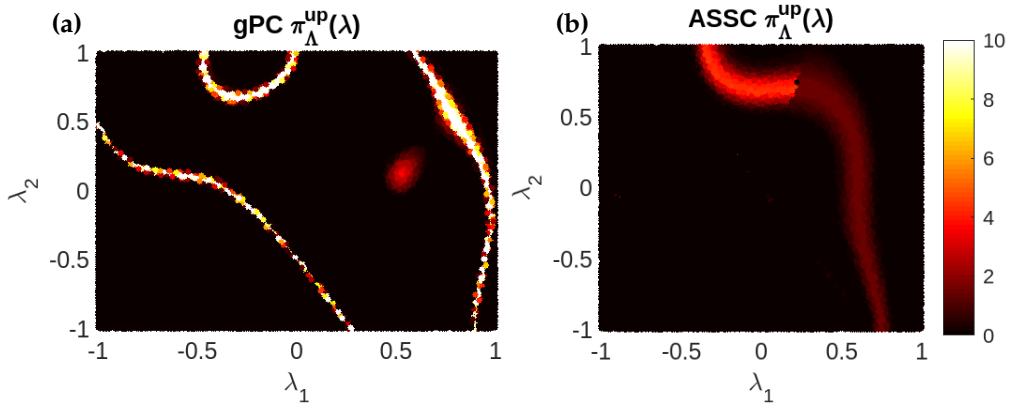

FIG. 3: *Verification. Updated density using rejection sampling algorithm on the metamodel: (a) Results using gPC metamodel, (b) Results using ASSC metamodel.*

The updated samples obtained using the rejection sampling algorithm for each of the metamodels are represented by red dots in Figure 2. The resulting updated probability densities π_Λ^{up} are illustrated in Figure 3 (a)-(b). We remark the updated probability densities are very different for each metamodel. Forward propagation of the updated density samples is performed next using both the metamodels and the analytical values of the QoI. The resulting push-forward probability densities π_D^{cons} (illustrated by green and red curves in Figure 4) are compared with the observed one. The gPC metamodel approximation led to an accurate inference result in its surrogate surface (see green curve on Figure 4 (a)). However, we can see in the same figure with the curve in red that the push-forward density using the analytical values (exact model) of the QoI is very much different from the observed one. This discrepancy can be explained by the QoI approximation by global polynomials, which does not take into account discontinuities while inferring. Moreover, the updated densities $\pi_\Lambda^{up}(\boldsymbol{\lambda})$ in Figure 3 (a)-(b) are very different for each metamodel which suggests the inference results are highly influenced by the metamodel choice.

The ASSC method presents as well an accurate inference result and shows an efficiency in detecting the singularities in the QoI domain. Indeed, both updated probability densities using the ASSC metamodel

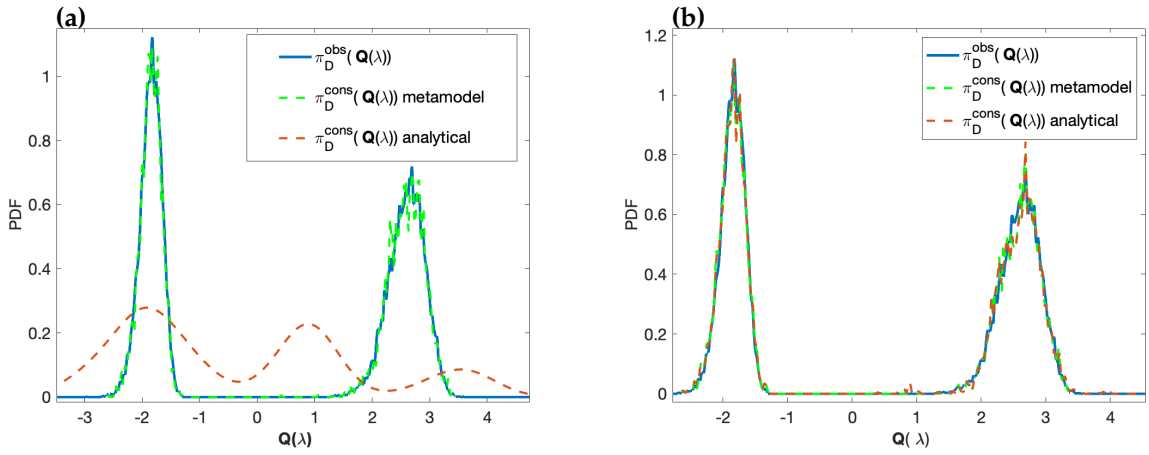

FIG. 4: *Verification: Updated push-forward densities results. Legend: (blue) observed (targeted) QoI density; (green) push-forward of the updated density using rejection sampling algorithm on the metamodel; (red) push-forward of the updated density using rejection sampling algorithm on the analytical (exact) model QoI. (a) Results using gPC metamodel. (b) Results using ASSC metamodel.*

and the analytical values of the QoI show a push-forward result close to the observed one (see Figure 4 (b)). These results show that the inference results are highly influenced by the metamodel choice and particularly we cannot neglect discontinuous behavior on the QoI map when solving stochastic inverse problems.

In Figure 5, we highlight the ASSC metamodel's capability for detecting discontinuities on the QoI space as opposed to a global polynomial approximation, where the QoI isolines for 10^5 samples evaluated from both gPC and ASSC metamodels are represented. We recall that the metamodel is built using an adaptive approach, where a stochastic error estimate is used as refinement criteria. This allows an automatic capturing of all (even highly anisotropic) discontinuities.

We can conclude that this analytical example comforts us in the choice of using the ASSC metamodel while solving the stochastic inverse problem, where an accurate inference result was obtained for a discontinuous QoI problem.

Thus, for the next two examples, we will build the metamodel using the ASSC method when solving the stochastic inverse problem.

6. COMPRESSIBLE CFD APPLICATIONS

The performance of the data-consistent inference method coupled with the adaptive stochastic collocation (ASSC) approach is tested here for two CFD compressible flow problems.
The deterministic solver considered here solves the compressible flow equations using a mixed finite volume - finite element formulation on unstructured triangular/tetrahedral meshes. A brief description of *WOLF* solver can be found in [42].

The two-dimensional steady Euler equations are set in the computational domain $\Omega \subset \mathbb{R}^2$ of boundary denoted Γ. We define our working functional space as $\mathcal{V} = \left[H^1(\Omega) \cap \mathcal{C}(\bar{\Omega})\right]^4$, that is the set of measurable functions that are continuous with square integrable gradient. We formulate the Euler model in a compact variational formulation in the functional space $\mathcal{V}$ as follows

$$\begin{aligned} &\text{Find } w \in \mathcal{V} \text{ such that } \forall \varphi \in \mathcal{V}, \quad (\Psi(w)\,,\,\varphi) = 0, \\ &\text{with} \quad (\Psi(w)\,,\,\varphi) \quad = \quad \int_\Omega \varphi\, \nabla \cdot \mathcal{F}(w)\, \mathrm{d}\Omega \;-\; \int_\Gamma \varphi\, \hat{\mathcal{F}}(w).\mathbf{n}\, \mathrm{d}\Gamma \;. \end{aligned} \tag{14}$$

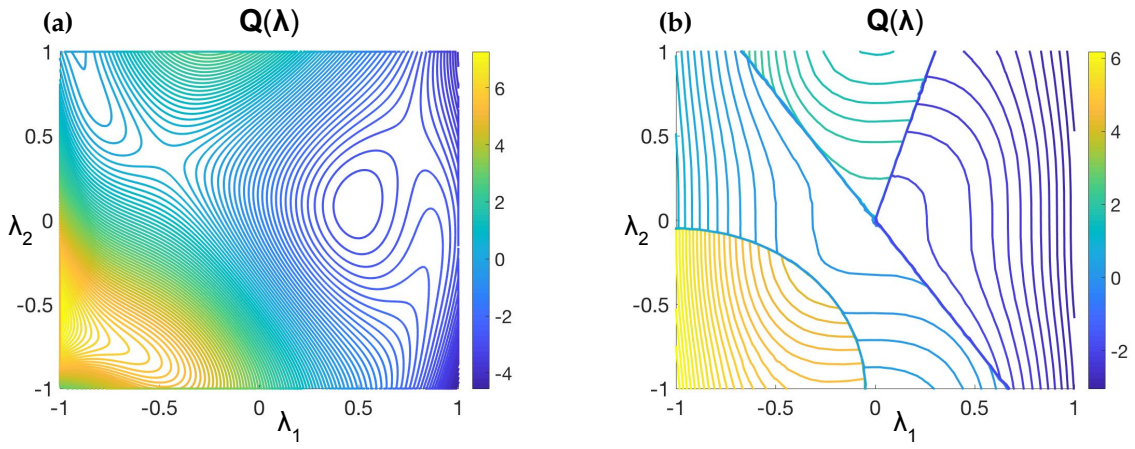

FIG. 5: *Verification. Iso-contours of the QoI evaluated with two forward propagation metamodels: (a) gPC (b) Adaptive Stochastic Collocation (ASSC)*

In the above definition, $w = {}^t(\rho,\ \rho\mathbf{u},\ \rho E)$ is the vector of conservative flow variables and $\mathcal{F}(w) = (\mathcal{F}_1(w), \mathcal{F}_2(w))$ is the usual Euler flux:

$$\mathcal{F}(w) = {}^t\left(\rho\mathbf{u},\ \rho u\mathbf{u} + p\mathbf{e}_x,\ \rho v\mathbf{u} + p\mathbf{e}_y,\ \rho\mathbf{u}H\right) .$$

We have noted ρ the fluid density, $\mathbf{u} = (u, v)$ the velocity vector, $H = E + p/\rho$ the total enthalpy, $E = T + \frac{\|\mathbf{u}\|^2}{2}$ the total energy, $p = (\gamma - 1)\rho T$ the pressure with $\gamma = 1.4$ the ratio of specific heat capacities, T the temperature, and $(\mathbf{e}_x, \mathbf{e}_y)$ the canonical basis.
Note that $\mathbf{n}$ is the outward normal to Γ, and the boundary flux $\hat{\mathcal{F}}$ contains the different boundary conditions, which involve standard inflow, outflow and slip boundary conditions.
The computational domain is then divided in a finite-element partition of simplicial (triangular) elements and the model (14) is discretized using a mixed finite-element/finite-volume approach on a discrete variational space. For further details on the discrete model, see [46]. This model is used for both CFD examples described hereafter.

6.1 Inviscid flow around a NACA0012 airfoil

The geometry considered for this example is a symmetric NACA0012 airfoil with chord length $c = 1$. The computational domain is discretized in an unstructured triangular mesh as shown in Figure 6 and the discrete Euler model is used to analyze the external compressible flow around the airfoil. The inflow conditions are defined by a free-stream Mach number M_∞ and an angle of attack α imposed upstream to our obstacle. The quantities of interest considered here, i.e. $\boldsymbol{Q}(\boldsymbol{\lambda}) = (Q_1(\boldsymbol{\lambda}), Q_2(\boldsymbol{\lambda}))$ are the point-wise Mach number values at coordinate $x/c = 0.25$ in the lower ($Q_1(\boldsymbol{\lambda})$) and respectively upper ($Q_2(\boldsymbol{\lambda})$) surfaces, with uncertain parameters $\boldsymbol{\lambda}$: the inflow conditions $\lambda_1 = M_\infty$ and $\lambda_2 = \alpha$. We consider thus the uncertain parameters domain $\Lambda = \{[0.5, 0.7] \times [2, 6]\}$. The pressure and respectively Mach fields for $M_\infty = 0.6$ and $\alpha = 4$ are illustrated in Figure 7. These values correspond to the middle of the uncertain parameters domain. We observe a small shock appear on the upper airfoil surface where the flow becomes supersonic and a non-symmetric solution due to a non-null value of the angle of attack. The free-stream Mach number M_∞ will have an influence on the intensity of this shock, while the angle of attack α will change the shock's position. For these particular values of the uncertain parameters, we observe our quantities of interest are either in a transsonic (for $Q_1(\boldsymbol{\lambda})$) or a subsonic (for $Q_2(\boldsymbol{\lambda})$) regime.

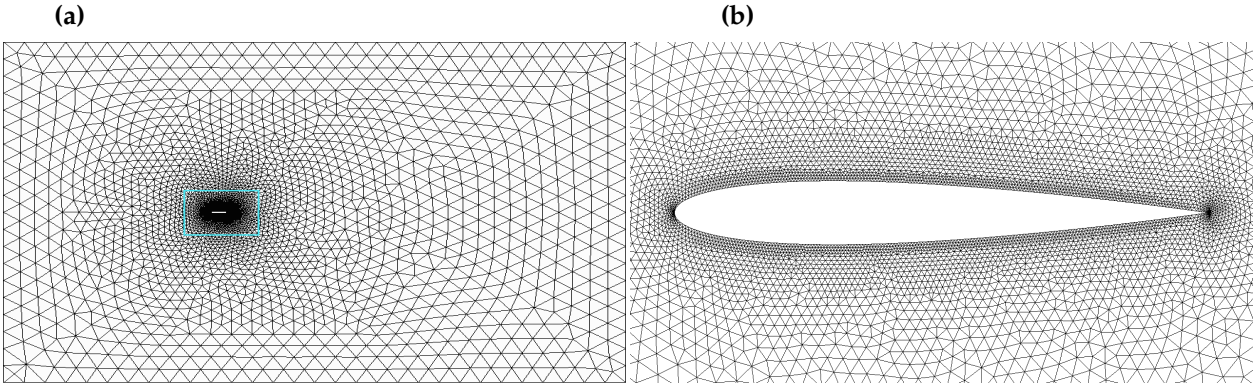

FIG. 6: *NACA0012 geometry and computational domain mesh.*

The observed (or targeted) data has been built using an initial probability density for our uncertain parameters and the forward (direct) propagation of these uncertainties throughout our Euler model. This allows us to control the types of flow we wish to analyze as summarized in Figure 8 where the domain (A) represents a subsonic flow and the domain (B) a transonic flow. A discontinuity is also represented on the QoI $Q_2(\boldsymbol{\lambda})$ map as shown in Figure 9 (left image), while the response surface of $Q_1(\boldsymbol{\lambda})$ is smooth (see right image of Figure 9).

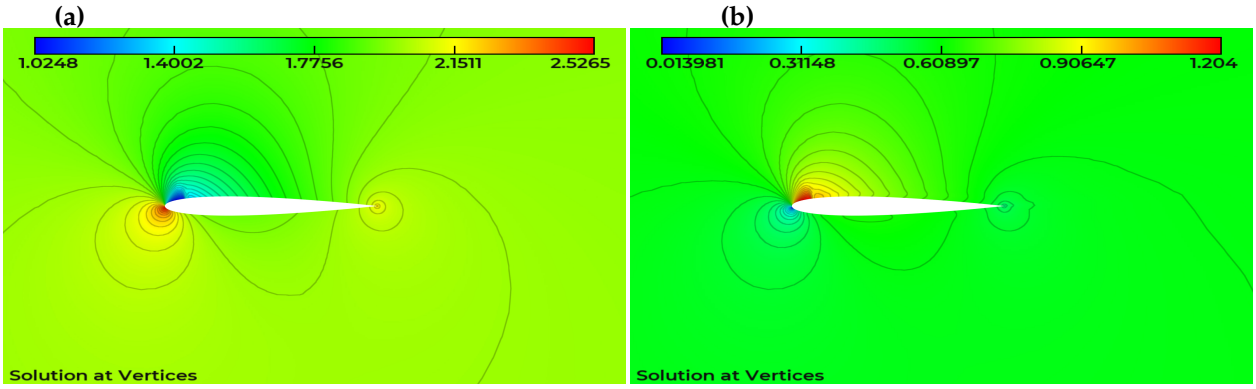

FIG. 7: *NACA0012. Pressure (left image) and Mach number (right image) fields for middle uncertain domain* Λ *values:* $M_\alpha = 0.6$ *and* $\alpha = 4$

For each of these studies, we compare the updated density and its push-forward with the observable π_D^{obs} and its support in Λ, π_Λ^{obs}. The data-consistent inference method is applied using the adaptive stochastic collocation metamodel with about 500 deterministic samples (CFD problems solves) and a LHS sampling over the metamodel is used to post-process the results. Figure 9 illustrates the response surface obtained for both QoI and again the capability of the adaptive approach to capture the discontinuity in Q_2.

Results for the subsonic case (A) are illustrated in Figures 10-11-12. The data-consistent inference led to a QoI pdf (see right image in Figure 11) in agreement with the observable (see left image in Figure 11) built with the support illustrated in left image (a) of Figure 10. Figure 12 illustrates the same results and conclusion with an individual view of each quantity of interest (results on $Q_1(\boldsymbol{\lambda})$ illustrated on the left image and on $Q_2(\boldsymbol{\lambda})$ on the right image). Moreover, the updated density illustrated in the right image of Figure 10 is of similar shape with the uniform support. We can conclude that for the subsonic case the inverse problem solution obtained using the data-consistent inference approach coupled with the adaptive stochastic collocation metamodel is accurate since the updated and push-forward densities are well reconstructed for our QoI $\boldsymbol{Q}(\boldsymbol{\lambda})$.

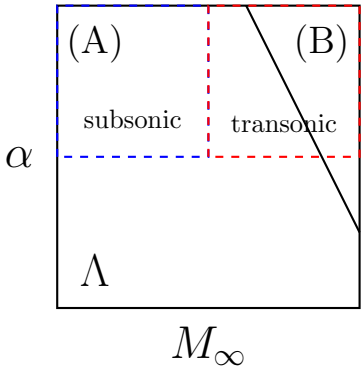

FIG. 8: *NACA0012. Stochastic supports (A) and (B) over the uncertain parameters space* Λ.

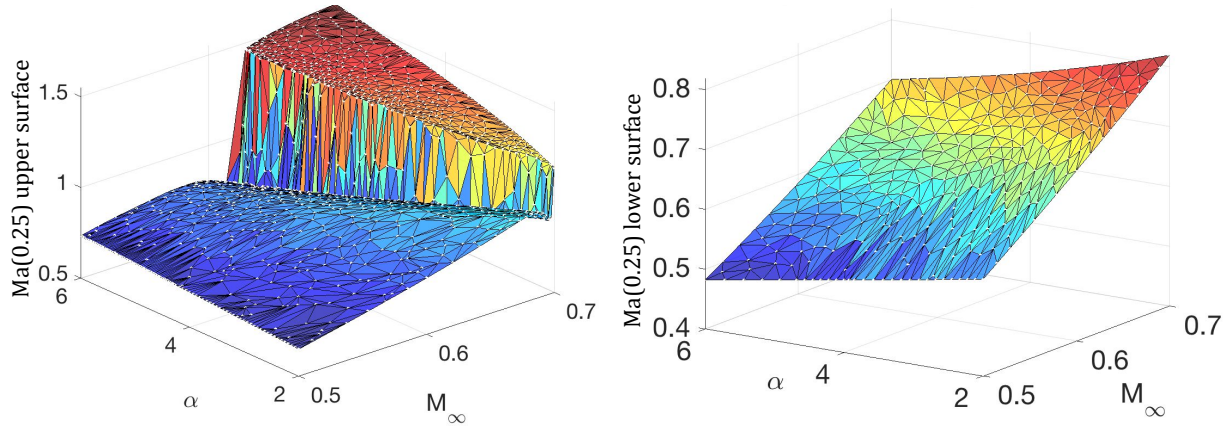

FIG. 9: *NACA0012. QoI response surfaces for both parameters support. 500 deterministic samples were used.*

When inferring on the data from the stochastic space in case (B) corresponding to the transonic flow with the data-generating density shown in Figure 13 (left), we see in Figures 14 and 15 that the push-forward of the updated density agrees very well with the observed pdf in each scenario. However, while the updated density illustrated in Figure 13 (right) presents a shape similar to the uniform support of the data-generating density shown in Figure 13 (left), some differences are notable. This discrepancy can be explained by a non-uniqueness of the inverse problem solution. When inferring the observed data, more than one density on Λ can push forward to the given observed density.

6.2 Inviscid flow in a Hyshot II-Scramjet configuration

Finally, the data-consistent inference is tested on an internal flow problem in a scramjet configuration. The geometry (illustrated in Figure (16)), flow conditions and the pseudo-combustion model were initially analyzed in [47] where the authors wished to assess the unstart condition on this problem using an adjoint-based approach for accelerating the Monte-Carlo method. Although the geometry is rather simple, the flow behavior is not. Indeed, this configuration is analyzed for a supersonic inflow Mach number M_∞ where the inlet velocity will always be parallel to the combustor walls. A shock train is generated by a blunt lip at the entrance of the lower wall of the isolator. The combustion will lead also to the entertainment of the shock train present in the combustor. In order to mimic the combustion process we added (as in [47]) a heat release model to the energy equation in the Euler model, defined by $S = \Phi f_{st} H_f m_{air} \eta(x/Lc)$,

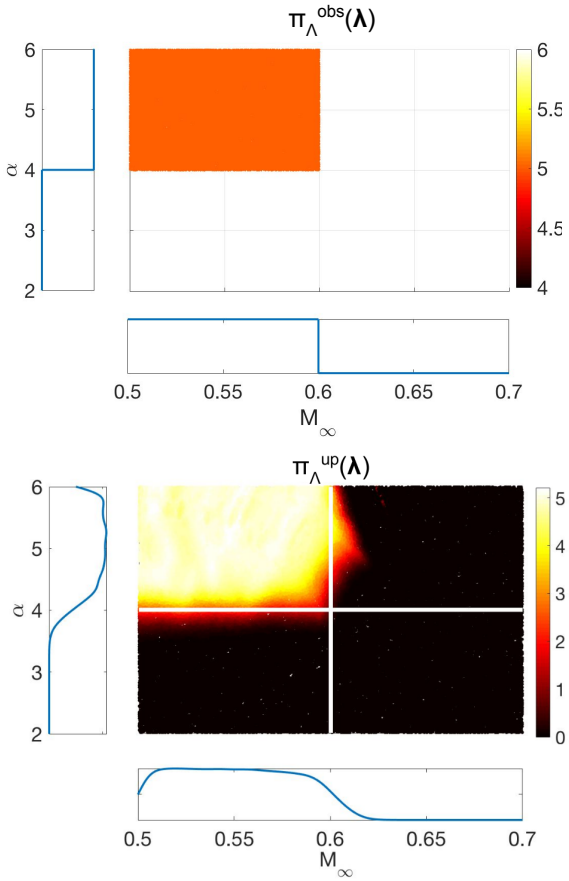

FIG. 10: *NACA0012. Data-generating probability density, π_Λ^{obs} (left), and the updated probability density, π_Λ^{up} (right), for case (A).*

with $\eta(x/Lc) = 1 - e^{-(C_c x/L_c)^{D_c}}$ the heat release distribution function and $C_c = -log(1 - K_c)^{D_c}$, where K_c is the *fraction of completed combustion* and D_c a shape parameter tuned to achieve a good fit with the ground-based experimental measurements. The remaining symbols represent: the equivalence ratio (Φ), the stoichiometric fuel/air ratio (f_{st}), the fuel heating value (H_f) and the mass of air (m_{air}). The quantity of interest is the normalized pressure deviation from the upstream pressure and is defined as follows:

$$\boldsymbol{Q}(\boldsymbol{\lambda}) = \left(\int_{\boldsymbol{\Gamma}} (p - p_\infty)^8 dx \right)^{1/8}. \tag{15}$$

We consider in this study two observation surfaces: the upper wall of the Hyshot scramjet combustor $\boldsymbol{\Gamma}$ (as shown in Figure 16) and the outflow O. Therefore, we introduce $\boldsymbol{Q}(\boldsymbol{\lambda}) = (Q_1, Q_2)$ with $Q_1(\boldsymbol{\lambda}) = \left(\int_\Gamma (p - p_\infty)^8 dx\right)^{1/8}$ and $Q_2(\boldsymbol{\lambda}) = \left(\int_O (p - p_\infty)^8 dx\right)^{1/8}$. By observing the QoI on these surfaces, we are able to predict the impact of several changes in the flow parameters on the train shock and thus incidentally on the unstart condition. This condition is characterized by a sudden drop of the system inlet flow velocity, which leads to the failure of the engine ignition.

We consider here two uncertain parameters: the fraction of complete combustion K_c and the free stream Mach number, M_∞, defined in $\Lambda = \{[0.8, 1] \times [2.8, 3.8]\}$. A stable solution is illustrated in Figure 17

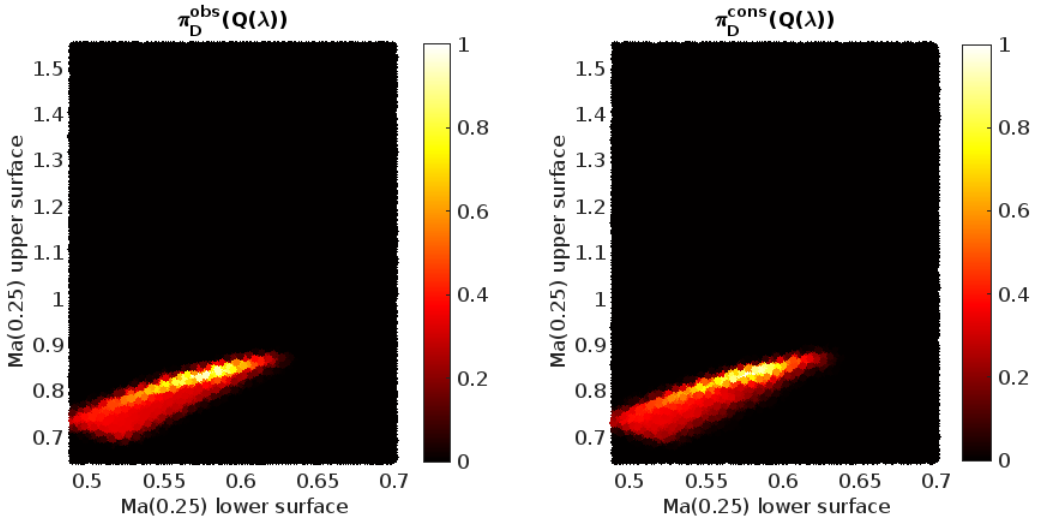

FIG. 11: *NACA0012. Normalized observed probability density, π_D^{obs} (left), and the normalized push-forward of the updated probability density, π_D^{cons} (right), for case (A) with two quantities of interest.*

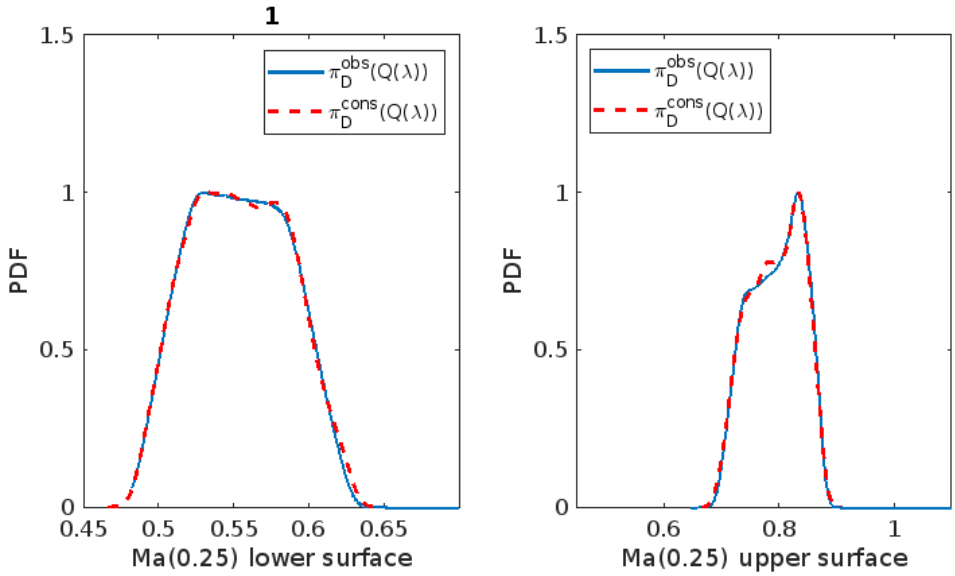

FIG. 12: *NACA0012. Normalized observed probability density, π_D^{obs}, and the normalized push-forward of the updated probability density, π_D^{cons}, for case (A) with one quantity of interest for the lower surface (left) and the upper surface (right).*

where the simulation has been performed for the middle values of the uncertain parameters: $M_\infty = 3.2$ and $K_c = 0.9$.

The observed data is built from a data-generating density, π_Λ^{obs}, within the uncertain parameters space, similarly to the previous CFD case. Two studies are conducted using two different data generating densities to build the observed data. First, we take π_Λ^{obs} to be a uniform density on part of the uncertain domain $\{[0,97, 1] \times [2.7, 2.9]\}$. In the second study, π_Λ^{obs} is a bivariate correlated Gaussian function centered at $\mu_1 = 0.9$ and $\mu_2 = 3.2$. For both studies, we start with a uniform distribution assumption of the uncertain parameters on Λ. The data-consistent inference method is then applied coupled with the ASSC metamodel

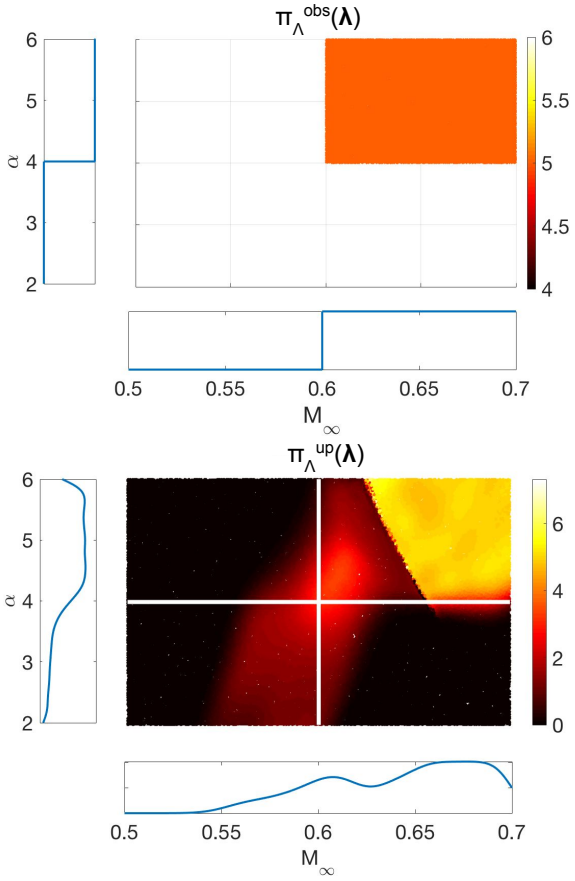

FIG. 13: *NACA0012. Data-generating probability density, π_Λ^{obs} (left), and the updated probability density, π_Λ^{up} (right), for case (B).*

built with 300 deterministic solves. For the post-processing, we used 2.10^5 LHS samples.

Successful results are obtained for both studies. We can see that the inference method is once again capable to accurately reconstruct the observed data and the density, π_Λ^{obs} meaning that the consistency with both the data and the model is verified. For the first study where a uniform support was defined, we can see in Figure 18 little differences with the updated density and π_Λ^{obs}. We see in Figures 19 and 20 that the push-forward of the updated density agrees very well with the observed pdf in each scenario. For the second, the Gaussian distribution is also well recovered in Λ (Figure 21). In the QoI space the inference method led again to an updated push forward density in agreement with the observed one, π_D^{obs} (see Figures 22 and 23).

These results confirm the good approximation of the QoI map by the ASSC metamodel and show the consistent inference capacity of reconstructing correlated support in the uncertain parameters space.

7. CONCLUSION

The data-consistent inference method was combined in this paper with an adaptive stochastic collocation (ASSC) approach to solve inverse stochastic CFD problems. The coupling of these methodologies allows addressing issues of both computational costs induced by solving expensive CFD inverse problems and

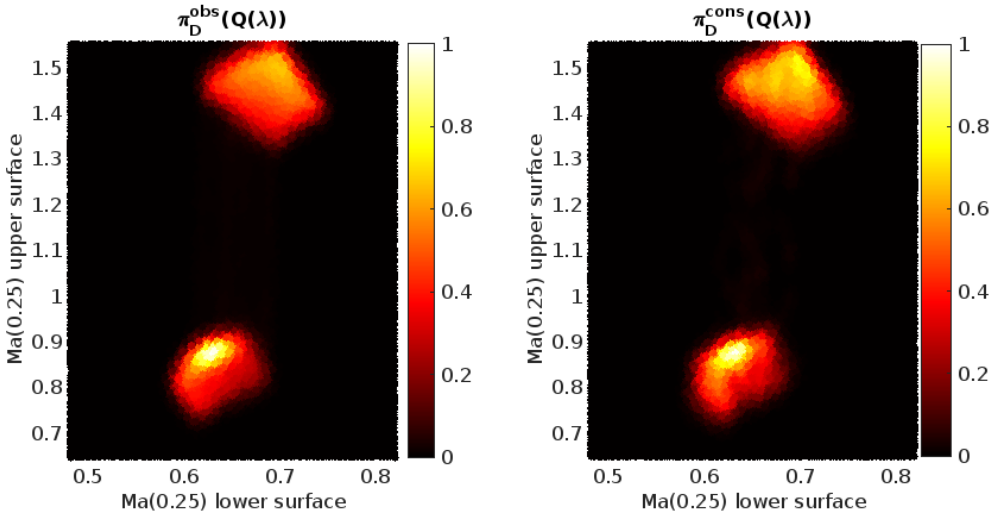

FIG. 14: *NACA0012. The normalized observed probability density, π_D^{obs} (left), and the normalized push-forward of the updated probability density, π_D^{cons} (right), for case (B) with two quantities of interest.*

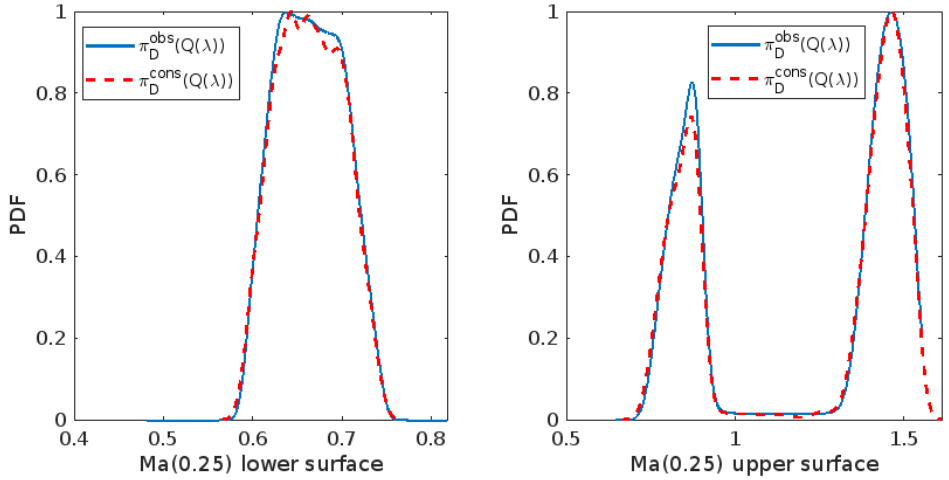

FIG. 15: *NACA0012. The normalized observed probability density, π_D^{obs}, and the normalized push-forward of the updated probability density, π_D^{cons}, for case (B) with one quantity of interest for the lower surface (left) and the upper surface (right).*

potentially discontinuous responses over the uncertain input parameters. A verification case with a discontinuous response surface showed the accuracy of this method to correctly catch the singularities in the QoI space, leading to correct inference results (36 deterministic samples were used). Results suggest that additional care may be taken when building the metamodel for this kind of problem.

Moreover, after the verification phase, the coupled tool was able to recover both 1D and 2D observed densities in the uncertain parameters and QoI stochastic spaces for two different CFD configurations, using an increasingly more complex model.

Of course, the inference results presented are also dependent on other factors not studied here, such as the kernel density estimation bandwidth, the QoI map, and other parameters we tuned. Such parametric studies could be the subject of a future work or further investigations, but this is beyond the scope of this article. Also, further studies shall focus on other forward propagation methods or metamodels, notably

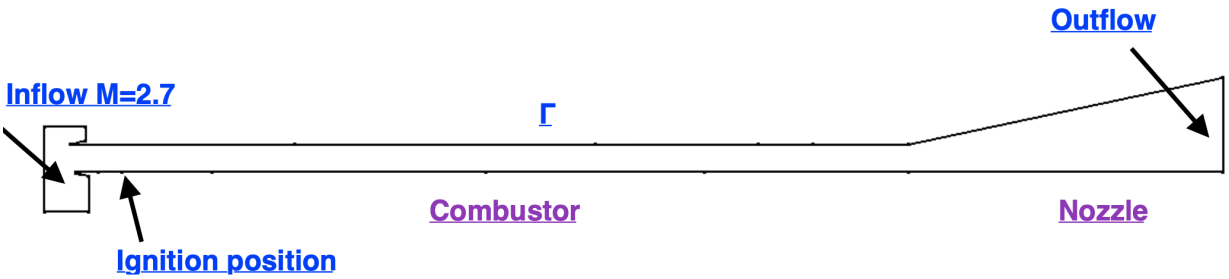

FIG. 16: *Hyshot II-Scramjet: geometry configuration and simulation domain.*

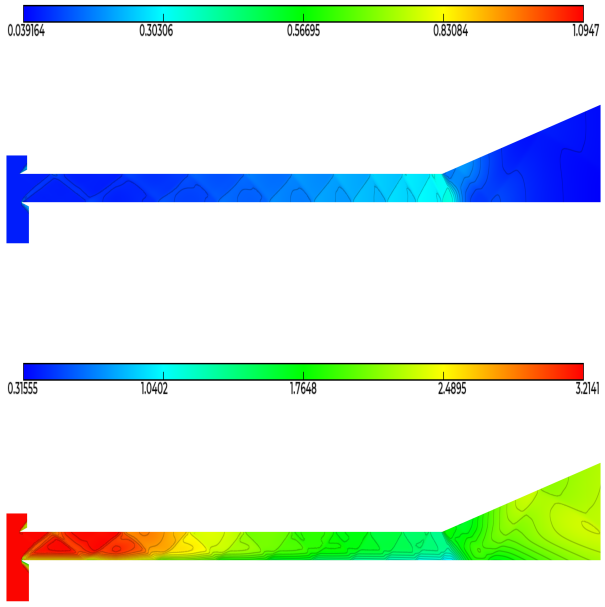

FIG. 17: *HyShot II-Scramjet. Pressure (left image) and Mach number (right image) fields for middle values of the uncertain parameter space* Λ*:* $M_\alpha = 3.2$ *and* $K_c = 0.9$

empirical ones, such as regressive neural networks, which might perform better in higher-dimensional parameter spaces.

ACKNOWLEDGMENTS

This article has been authored by an employee of National Technology & Engineering Solutions of Sandia, LLC under Contract No. DE-NA0003525 with the U.S. Department of Energy (DOE). The employee owns all right, title and interest in and to the article and is solely responsible for its contents. The United States Government retains and the publisher, by accepting the article for publication, acknowledges that the United States Government retains a non-exclusive, paid-up, irrevocable, world-wide license to publish or reproduce the published form of this article or allow others to do so, for United States Government purposes. The DOE will provide public access to these results of federally sponsored research in accordance

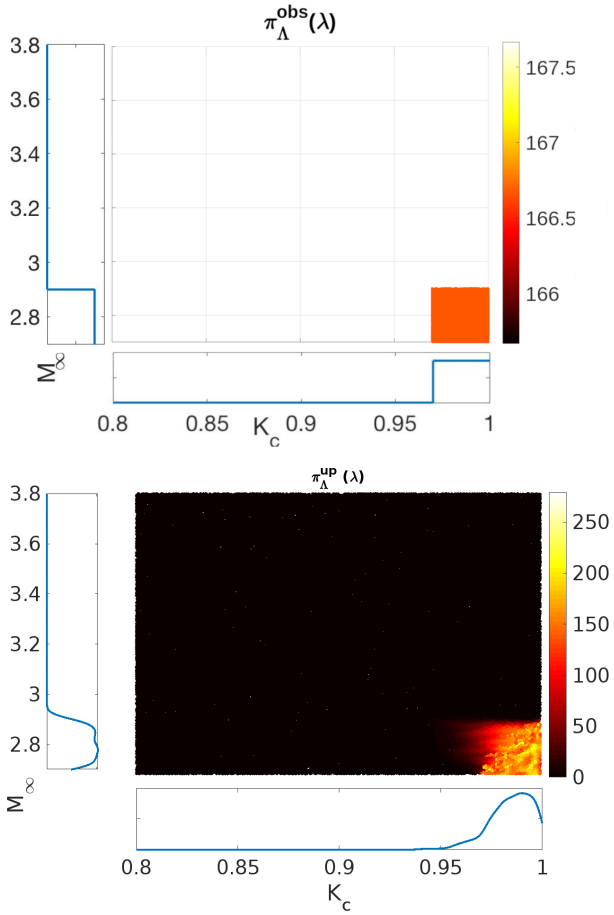

FIG. 18: *HyShot II-Scramjet. Data-generating density, π_Λ^{obs} (left), and the updated probability density, π_Λ^{up} (right), for the first scramjet case.*

with the DOE Public Access Plan https://www.energy.gov/downloads/doe-public-access-plan. This paper describes objective technical results and analysis. Any subjective views or opinions that might be expressed in the paper do not necessarily represent the views of the U.S. Department of Energy or the United States Government.

REFERENCES

1. Xiu, D. and Karniadakis, G., The Wiener–Askey polynomial chaos for stochastic differential equations, *SIAM J. Sci. Comput.*, 24:619–644, 2002.
2. Babuška, I., Nobile, F., and Tempone, R., A stochastic collocation method for elliptic partial differential equations with random input data, *SIAM J. Numer. Analysis*, 45:1005–1034, 2007.
3. Xiu, D. and Hesthaven, J., High-order collocation methods for differential equations with random inputs, *SIAM J. Sci. Comput.*, 27:1118–1139, 2005.
4. Bijl, H., Lucor, D., Mishra, S., and Schwab, C. (Eds.), *Uncertainty quantification in Computational Fluid Dynamics*, Vol. 92 of Lecture Notes in Computational Science and Engineering, Springer, 2013.
5. Abgrall, R. and Mishra, S. Uncertainty quantification for hyperbolic systems of conservation laws. In *Handbook*

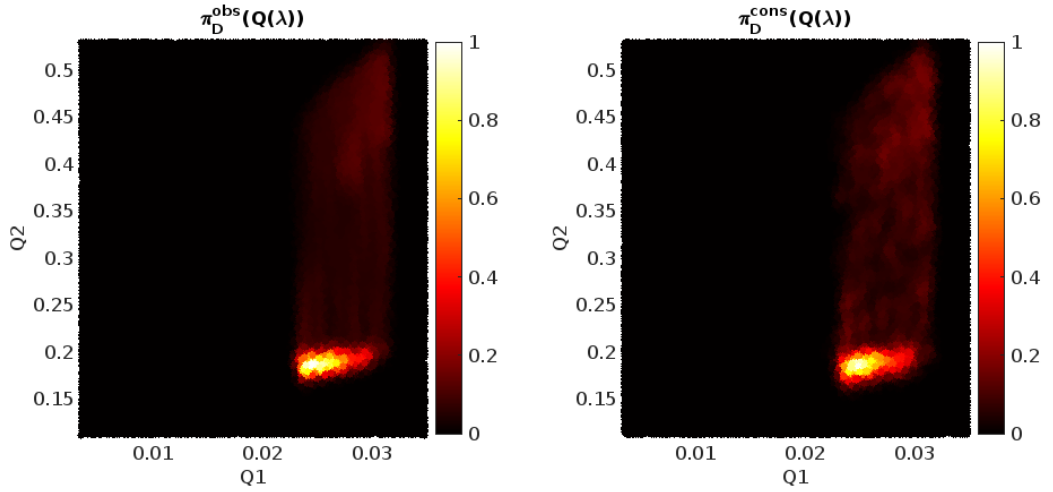

FIG. 19: *HyShot II-Scramjet. The normalized observed probability density, π_D^{obs} (left), and the normalized push-forward of the updated probability density, π_D^{cons} (right), for the first scramjet case with two quantities of interest.*

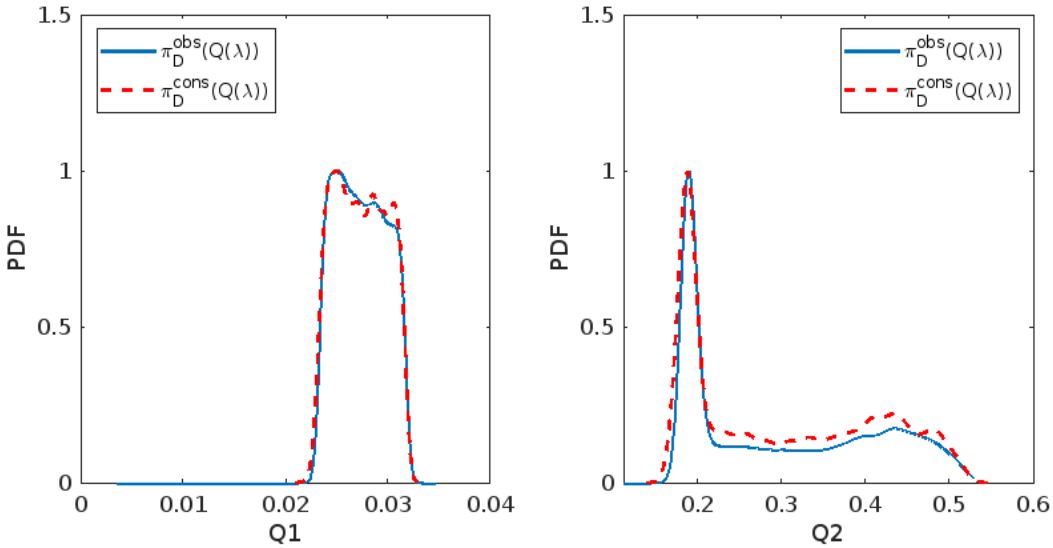

FIG. 20: *HyShot II-Scramjet. The normalized observed probability density, π_D^{obs}, and the normalized push-forward of the updated probability density, π_D^{cons}, for the first scramjet case with each quantity of interest inferred separately.*

of Numerical Methods for Hyperbolic Problems, Vol. 18 of Handbook of Numerical Analysis, chapter 19, pp. 507–544. Elsevier, 2017.

6. Poette, G. and Lucor, D., Non-intrusive iterative stochastic spectral representation with application to compressible gas dynamics, *Journal of Computational Physics*, 231(9):3598–3609, 2012.
7. Nobile, F., Tempone, R., and Webster, C., An anisotropic sparse grid stochastic collocation method for partial differential equations with random input data, *SIAM J. Numer. Analysis*, 46(5):2411–2442, 2008.
8. Wan, X. and Karniadakis, G., An adaptive Multi-Element generalized polynomial chaos method for stochastic differential equations, *Journal of Computational Physics*, 209(2):617–642, 2005.

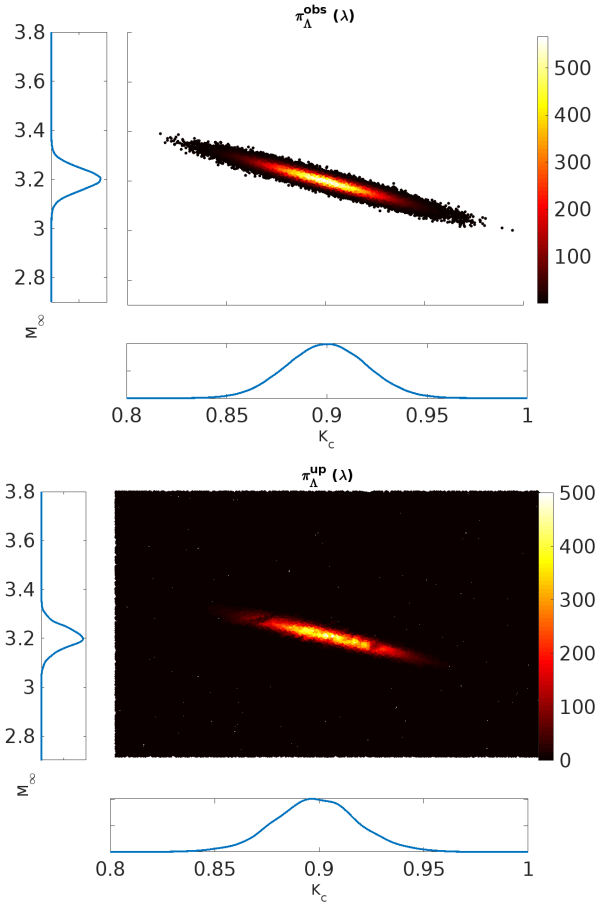

FIG. 21: *HyShot II-Scramjet. Data-generating density, π_Λ^{obs} (left), and the updated probability density, π_Λ^{up} (right), for the second scramjet case.*

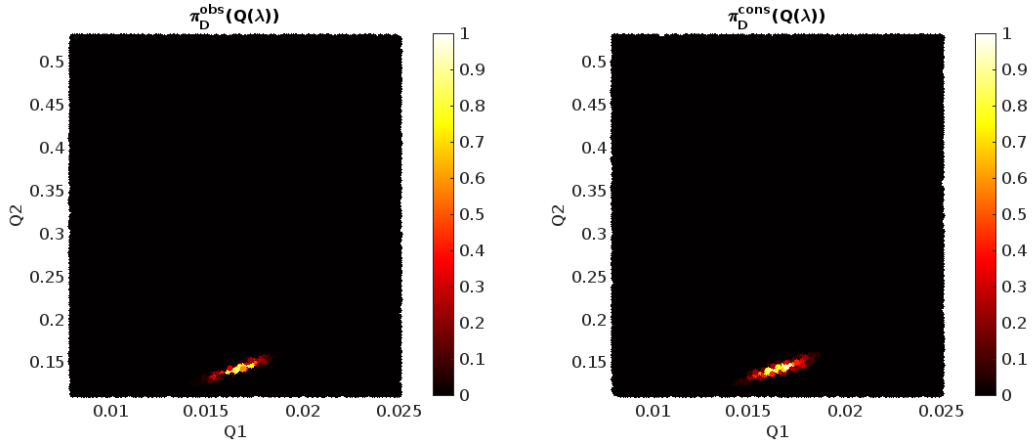

FIG. 22: *HyShot II-Scramjet. The normalized observed probability density, π_D^{obs} (left), and the normalized push-forward of the updated probability density, π_D^{cons} (right), for the second scramjet case with two quantities of interest.*

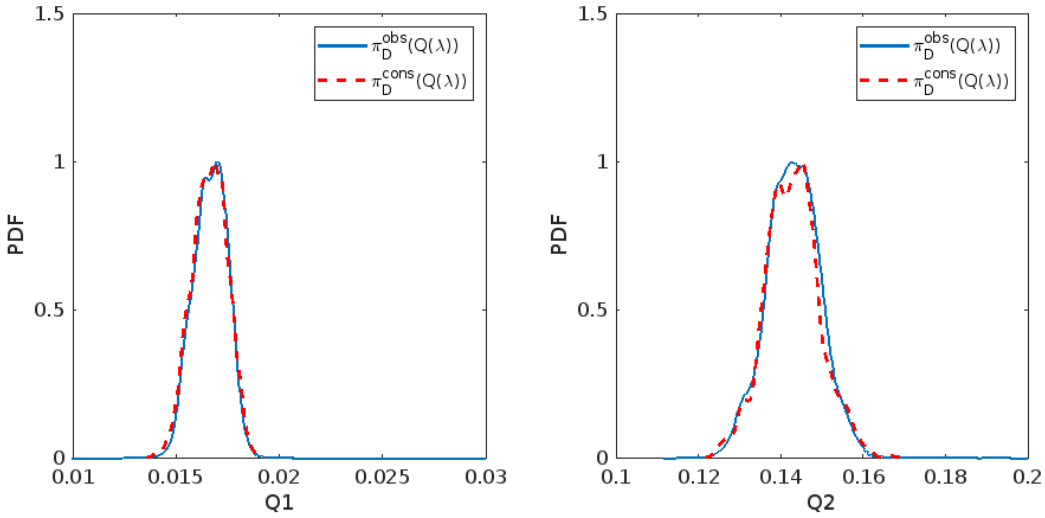

FIG. 23: *HyShot II-Scramjet. The normalized observed probability density, π_D^{obs}, and the normalized push-forward of the updated probability density, π_D^{cons}, for the second scramjet case with each quantity of interest inferred separately.*

9. Foo, J. and Karniadakis, G., Multi-element probabilistic collocation method in high dimensions, *Journal of Computational Physics*, 229(5):1536–1557, 2010.
10. Bryant, C., Prudhomme, S., and Wildey, T., Error decomposition and adaptivity for response surface approximations from PDEs with parametric uncertainty, *SIAM/ASA Journal on Uncertainty Quantification*, 3(1):1020–1045, 2015.
11. Jakeman, J., Narayan, D., and Xiu, D., Minimal Multi-Element stochastic collocation for uncertainty quantification of discontinuous functions, *Journal of Computational Physics*, 242:790–808, 2013.
12. Le Maıtre, O., Najm, H., Ghanem, R., and Knio, O., Multi-resolution analysis of wiener-type uncertainty propagation schemes, *Journal of Computational Physics*, 197(2):502–531, 2004.
13. Archibald, R., Gelb, A., Saxena, R., and Xiu, D., Discontinuity detection in multivariate space for stochastic simulations, *Journal of Computational Physics*, 228(7):2676–2689, 2009.
14. Bernardo, J. and Adrian, F., *Bayesian Theory*, Wiley, Chichester, 1994.
15. Kaipio, J. and Somersalo, E., Statistical inverse problems: Discretization, model reduction and inverse crimes, *Journal of Comp. Appl. Math.*, 198:493–504, 2007.
16. Marzouk, Y.M., Najm, H.N., and Rahn, L.A., Stochastic spectral methods for efficient bayesian solution of inverse problems, *Journal of Computational Physics*, 224(2):560–586, 2007.
17. Marzouk, Y.M. and Xiu, D., A stochastic collocation approach to bayesian inference in inverse problems, *Cpmmun. Comput. Physics*, 6(4):826–847, 2009.
18. Marzouk, Y.M. and Najm, H.N., Dimensionality reduction and polynomial chaos acceleration of bayesian inference in inverse problems, *Journal of Computational Physics*, 228(6):1862–1902, 2009.
19. Tarantola, A., *Inverse Problem Theory and Methods for Model Parameter Estimation*, SIAM, 2005.
20. Yan, L. and Zhou, T., Adaptive multi-fidelity polynomial chaos approach to bayesian inference in inverse problems, *Journal of Computational Physics*, 381:110–128, 2019.
21. Prudhomme, S. and Bryant, C.M., Adaptive surrogate modeling for response surface approximations with application to bayesian inference, *Advanced Modelling and Simulation in Engineering Sciences*, 2:1–21, 2015.
22. Butler, T., Jakeman, J., and Wildey, T., Combining push-forward measures and bayes rule to construct consistent solutions to stochastic inverse problems, *SIAM. J. Sci. Comput.*, 40:A984–A1011, 2018.

23. Butler, T., Wildey, T., and Yen Tian, Y., Data-consistent inversion for stochastic input-to-output maps. inverse problems, *Inverse Problems*, 36(8), 2020.
24. Butler, T., Jakeman, J., and Wildey, T., Optimal experimental design for prediction based on push-forward probability measures, *Journal of Computational Physics*, 416, 2020.
25. Butler, T., Jakeman, J., and Wildey, T., Convergence of probability densities using approximate models for forward and inverse problems in uncertainty quantification, *SIAM J. Sci. Comput.*, 40:A3523–A3548, 2020.
26. Tran, A. and Wildey, T., Solving stochastic inverse problems for property-structire linkages using data-consistent inversion and machine learning, *JOM*, 73:72–89, 2021.
27. Van Langenhove, J., Lucor, D., Alauzet, F., and Belme, A., Goal-oriented error control of stochastic system approximations using metric-based anisotropic adaptations, *Journal of Computational Physics*, 374:384–412, 2018.
28. Butler, T., Wildey, T., and Zhang, W., l^p convergence of approximate maps and probability densities for forward and inverse problems in uncertainty quantification, *International Journal for Uncertainty Quantification*, 12(4):65–92, 2022.
29. Dellacherie, X. and Meyer, P., *Probabilities and Potential*, North-Holland Publishing Co., 1979.
30. Butler, T., Estep, D., Tavener, S., Dawson, C., and Westerink, J.J., A measure-teoretic computational method for inverse sensitivity problems iii: Multiple quantities of interest, *SIAM/ASA Journal on Uncertainty Quantification*, 2:174–202, 2014.
31. Wan, X. and Karniadakis, G., Multi-element generalized polynomial chaos for arbitrary probability measures, *SIAM Journal on Scientific Computing*, 28(3):901–928, 2006.
32. Witteveen, J.A. and Iaccarino, G., Simplex stochastic collocation with eno-type stencil selection for robust uncertainty quantification, *Journal of Computational Physics*, 239:1–21, 2013.
33. Langenhove, J.V., Adaptive control of deterministic and stochastic approximation errors in simulations of compressible flow, PhD thesis, Université Pierre et Marie Curie (Paris VI), Paris, France, 2017.
34. Loseille, A., Dervieux, A., Frey, P., and Alauzet, F., Achievement of global second-order mesh convergence for discontinuous flows with adapted unstructured meshes, In *37th AIAA Fluid Dynamics Conference and Exhibit*, AIAA-2007-4186, Miami, FL, USA, Jun 2007.
35. Alauzet, F. and Loseille, A., High order sonic boom modeling by adaptive methods, *Journal of Computational Physics*, 229:561–593, 2010.
36. Belme, A., Dervieux, A., and Alauzet, F., Time accurate anisotropic goal-oriented mesh adaptation for unsteady flows, , 231(19):6323–6348, 2012.
37. Loseille, A. and Alauzet, F., Continuous mesh framework. Part I: well-posed continuous interpolation error, *SIAM J. Numer. Analysis*, 49(1):38–60, 2011.
38. Loseille, A. and Alauzet, F., Continuous mesh framework. Part II: validations and applications, *SIAM J. Numer. Analysis*, 49(1):61–86, 2011.
39. Witteveen, J., Loeven, A., and Bijl, H., An adaptive stochastic finite elements approach based on Newton–Cotes quadrature in simplex elements, *Computers & Fluids*, 38(6):1270–1288, 2009.
40. Witteveen, J. and Iaccarino, G., Simplex stochastic collocation with random sampling and extrapolation for non-hypercube probability spaces, *SIAM J. Sci. Comput.*, 34(2):A814–A838, 2012.
41. Loseille, A., Adaptation de maillage anisotrope 3D multi-échelles et ciblée à une fonctionnelle pour la mécanique des fluides. Application à la prédiction haute-fidélité du bang sonique, PhD thesis, INRIA, Paris, France, 2008. (in French).
42. Alauzet, F. and Loseille, A., A decade of progress on anisotropic mesh adaptation for computational fluid dynamics, *Computers & Design*, 72:13–39, 2016.
43. George, P., Hecht, F., and Vallet, M., Creation of internal points in Voronoi's type method. Control adaptation, *Advances in engineering software and workstations*, 13(5-6):303–312, 1991.
44. Alauzet, F. and Loseille, A., Metrix user guide. error estimates and mesh control for anisotropic mesh adaptation, Tech. Rep., INRIA, 2009.
45. Loseille, A. and Löhner, R., Adaptive anisotropic simulations in aerodynamics, In *48th AIAA Aerospace Sciences*

Meeting Including the New Horizons Forum and Aerospace Exposition, AIAA-2010-169, Orlando, FL, USA, Jan. 2010.

46. Belme, A., Aérodynamique instationnaire et méthode adjointe, PhD thesis, Université de Nice Sophia Antipolis, Sophia Antipolis, France, 2011. (in French).
47. Wang, Q., Duraisamy, K., Alonso, J., and Iaccarino, G., Risk assessment of scramjet unstart using adjoint-based sampling methods, *AIAA Journal*, 50, 2012.